enhancement ($n = 3$), or had a drainage tube ($n = 1$) or aneurysm clip ($n = 1$). The remaining 20 patients consisted of 11 men (mean age, 63 years) and nine women (mean age, 62 years), with a median age of 64 years (range, 35–82 years).

In 12 of the 20 patients, one of the attending neuroradiologists (nonauthor) saw early signs of acute ischemic stroke on nonenhanced CT, CT angiographic, and/or CT perfusion images. Most of the lesions were small and included areas of low attenuation and signs of highly attenuating vessels on the nonenhanced CT images. In one patient, a large infarct was seen in the middle cerebral artery on both the nonenhanced CT and CT angiographic images, and in two patients, perfusion defects were visible on the CT perfusion maps. In eight of 20 patients, no signs of stroke were visible on CT, CT angiographic, or CT perfusion images. One neuroradiologist (nonauthor, with 10 years of experience) retrospectively reevaluated the data from the 20 patients for signs of stroke.

Imaging was performed with a 320–detector row CT scanner (Toshiba Aquilion ONE; Toshiba Medical Systems, Otawara, Japan). A bolus of 50 mL of nonionic contrast agent with 300 milligrams of iodine per milliliter (Xenetix 300; Guerbet, Paris, France) was injected into an antecubital vein at a rate of 5 mL/sec followed by a 40-mL saline flush at the same rate. The CT perfusion protocol was started 5 seconds after contrast fluid injection, with a high-dose volumetric scan at 200 mAs, followed after 4 seconds by 13 scans, one every 2 seconds, at 100 mAs, then by five scans, one every 5 seconds, at 75 mAs. The total scan duration was less than 1 minute and the total exposure was 1875 mAs. Each volumetric scan had 16-cm coverage and was performed at 80 kV with a rotation time of 0.5 second. Reconstructions were performed with a smooth convolution kernel (FC41) and the reconstructed images had a resolution of 512 × 512 × 320 pixels and voxel sizes of 0.47 × 0.47 × 0.5 mm. The 19 volumes of the CT perfusion protocol were rigidly registered to the first time point to correct for possible patient movement (9,10). The average ± standard deviation effective dose was 5.0 mSv ± 0.2, reported according to the International Electrotechnical Commission standards, edition 3.0 (11).

Digital Phantoms

To study the influence of dose reduction on the calculated perfusion values, it is necessary to use exposure settings other than those used in the original protocol for each patient. However, this presents ethical and practical concerns, because an estimated 1.9 million neurons are lost every minute brain tissue is deprived of blood (12), rendering any subsequent acquisition to be a different snapshot in time. Therefore, patient imaging data obtained with the original scan protocol were used as starting points for simulation of scan protocols at lower total exposure. To simulate a scan at another dose level effectively, patient-specific digital phantoms were built.

The digital phantoms consisted of three elements: spatial content (the three-dimensional information), measured tissue attenuation curves (the four-dimensional information), and measured noise. The spatial content was a presegmented MR imaging brain atlas that was publicly available and that allowed definition of white matter, gray matter, and cerebrospinal fluid (13) combined with a skull and two cylinders to represent the anterior and posterior brain for artery and vein definition, respectively. Tissue curves were measured in the patient data by using regions of interests in the normal-appearing white matter and the normal-appearing basal ganglia in the M1 segment of the middle cerebral artery in the unaffected side and in the sinus sagittalis superior. These were annotated on 5-mm slabs of the temporal average image and maximum intensity projection image by one observer (M.T.H.O., with 4 years of experience). The average curve of each tissue type was taken as a proxy of a noise-free representation and was assigned to the corresponding locations in the digital phantoms. Noise was measured by scanning an anthropomorphic skull phantom at 23 different exposure settings of 10–230 mAs. At each setting, 31 scans were performed to capture the random variation of noise. Between each scan, we let the CT tube cool down to standard operating temperature. All other settings of these volumetric acquisitions were the same as those in the patient protocol. Each time point of the digital phantoms was randomly assigned a noise scan at one of these exposure settings to simulate a new CT perfusion protocol. The resulting digital phantoms were cropped to 8-cm coverage to reduce computation time and were resampled to a slab thickness of 5 mm. An example of a digital phantom constructed from patient tissue curves and their corresponding CBF maps is shown in Figure 1. We referred to an article by van den Boom et al (14) for detailed background and validation of these phantoms. Our digital phantom framework is available online (*http://digitalphantom.diagnijmegen.nl/*).

Protocol Simulations

A total of 10 CT perfusion protocols were simulated for each patient, with total radiation exposure decreasing by 10% with each step. The maximum total exposure was 1875 mAs (100%) and the lowest exposure was 190 mAs (approximately 10%) for the 19 time points. For each total exposure setting and for each patient, 10 random permutations were simulated after a uniform distribution of the protocol to capture the random variations of noise. Thus a total of 20 × 10 × 10 = 2000 CT perfusion protocols were simulated (ie, 2000 four-dimensional digital phantoms were built).

Perfusion Analysis

CBF, CBV, and MTT maps of each digital phantom were calculated by using perfusion analysis software (Perfusion Mismatch Analyzer, version 5.0; Acute Stroke Imaging Standardization Group, Japan, *http://asist.umin.jp/index-e.htm*). We selected the delay-insensitive block-circulant singular value decomposition method (15), a 256 × 256 matrix, and 5-mm slabs, smoothing turned on,

Figure 1

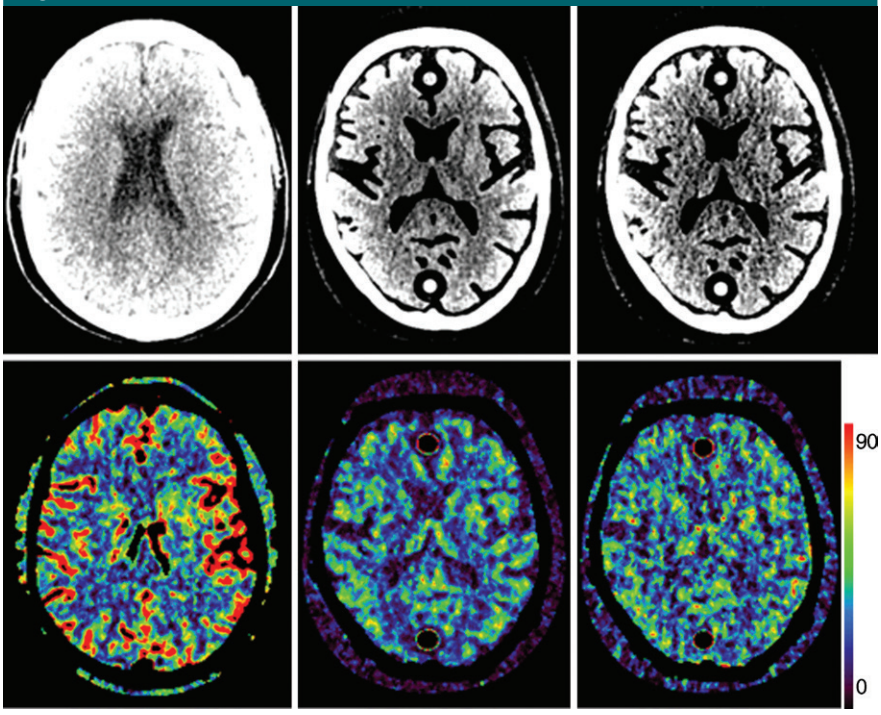

Figure 1: Pairwise CT perfusion images and corresponding CBF maps in a 60-year-old man with clinical symptoms of acute ischemic stroke include CT perfusion image (upper left) acquired with total dose of 5.0 mSv (100%) and corresponding CBF map (lower left), digital phantom constructed from patient white matter and basal ganglia tissue curves at same dose settings (upper middle) and corresponding CBF map (lower middle), and finally digital phantom from same tissue curves at 2.0 mSv (40%, upper right) of the total dose and corresponding CBF map (lower right). Window width and level settings were 50 HU and 40 HU, respectively. Perfusion maps were calculated by using block-circulant singular value decomposition method with perfusion mismatch analyzer from the Acute Stroke Imaging Standardization Group.

default parameters, and arterial input function rescaling with the venous output function. The other parameter settings of the perfusion mismatch analyzer were kept at default values.

Data Analysis

For each dose percentage setting and for each patient, 10 different phantoms were created, with random noise permutations. The mean ± standard deviation of the perfusion values of the 10 phantoms were taken as the representative perfusion value and representative noise in the perfusion image for that particular dose percentage setting and patient. At a patient level, there were six mean perfusion values and corresponding standard deviations (CBF, CBV, and MTT for both white matter and gray matter).

At the patient group level, for each dose percentage setting, the mean ± standard deviation perfusion values per tissue type were plotted as a function of the dose percentage setting for visualization of the average trend. Thus six mean and corresponding standard deviations representing patient variability were plotted as functions of dose levels. The lowest percentage setting for which the difference from that of the reference standard remained within 5% was marked as optimal.

Statistical Analysis

Bland and Altman analyses were performed to compare the perfusion values at the 5.0-mSv reference standard dose with the perfusion values at lower doses. The Pearson correlation coefficient was used to assess correlation between values at the optimal setting and the reference values. The slope of the linear fit between the optimal setting and the reference standard were reported. Shapiro-Wilk tests were performed to test the normality of the distributions of the differences, and paired *t* tests were performed to compare means. Two-tailed statistical tests were used, with a *P* value less than .05 indicating a significant difference. All statistical analyses were performed by using statistical software (Statistical Package of Social Sciences version 20.0 for Windows; SPSS, Chicago, Ill).

Results

Figure 2 shows the trends of CBF, CBV, and MTT as functions of the dose percentage setting, with error bars indicating patient variability. Patient variability was relatively constant. At 2.5 mSv, the maximum mean differences from the reference standard were 4.5%, 5.0%, and 1.9%, for CBF, CBV, and MTT, respectively. This point was selected as the optimal dose setting.

Table 1 shows the bias, standard deviations of the differences, and the limits of agreement as 95% confidence intervals for the patient perfusion values compared with the reference standard for white matter and gray matter combined. For dose reductions up to 2.5 mSv, the standard deviations, and therefore, the limits of agreement, remained small, and all biases remained close to zero. At the optimal setting, the mean ± standard deviation differences and limits of agreement were 0.4 mL/min per 100 g ± 2.8 (95% confidence interval: −5.1, 6.0) for CBF, 0.0 mL/100 g ± 0.2 (95% confidence interval: −0.3, 0.3) for CBV, and 0.1 sec ± 0.3 (95% confidence interval: −0.5, 0.7) for MTT.

The patient perfusion values at the optimal setting and the values of the reference standard are shown in scatterplots (Fig 3). Linear fits with zero intercept show slope values close to the ideal value of 1.0 (range, 1.00–1.02 [Fig 3]), and correlation was high, with Pearson correlation coefficients

Figure 2

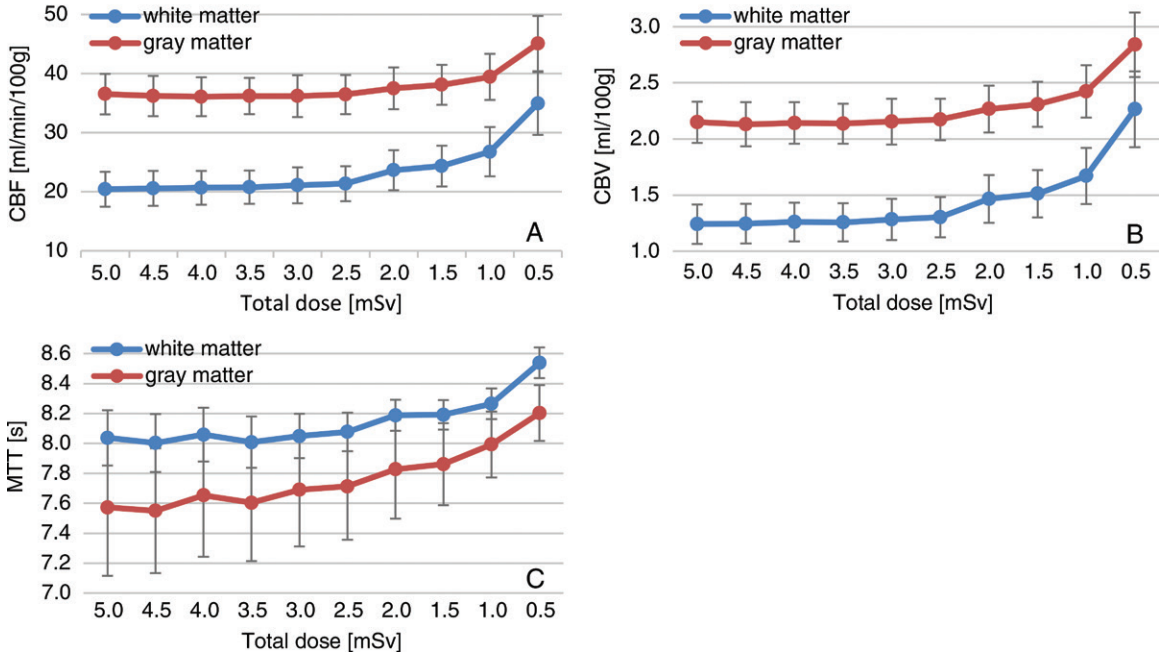

Figure 2: Graphs show perfusion values (CBF, CBV, and MTT) as function of total dose. Patient variability was relatively constant and there was marked increase in perfusion values, in particular for white matter, from 2.0 mSv and lower. Maximum mean differences for both white matter and gray matter between 5.0 mSv and 2.5 mSv doses were 4.5% for CBF, 5.0% for CBV and 1.9% for MTT. At 2.0 mSv, these were 15.6%, 18.1%, and 3.4%, respectively.

Table 1

Differences of Perfusion Values Compared with Reference Standard at 5.0 mSv

Total Dose (mSv)	CBF	CBV	MTT
4.5	−0.1 ± 2.3 (−4.7, 4.5)	0.0 ± 0.1 (−0.3, 0.3)	0.0 ± 0.2 (−0.5, 0.4)
4.0	−0.1 ± 2.6 (−5.2, 4.9)	0.0 ± 0.2 (−0.3, 0.3)	0.1 ± 0.2 (−0.4, 0.5)
3.5	0.0 ± 2.7 (−5.4, 5.4)	0.0 ± 0.2 (−0.3, 0.3)	0.0 ± 0.3 (−0.6, 0.6)
3.0	0.2 ± 2.7 (−5.1, 5.4)	0.0 ± 0.2 (−0.3, 0.3)	0.1 ± 0.3 (−0.5, 0.6)
2.5	0.4 ± 2.8 (−5.1, 6.0)	0.0 ± 0.2 (−0.3, 0.3)	0.1 ± 0.3 (−0.5, 0.7)
2.0	2.1 ± 4.2 (−6.2, 10.3)	0.2 ± 0.2 (−0.3, 0.6)	0.2 ± 0.4 (−0.5, 0.9)
1.5	2.7 ± 3.8 (−4.7, 10.1)	0.2 ± 0.2 (−0.1, 0.6)	0.2 ± 0.4 (−0.6, 1.0)]
1.0	4.6 ± 6.2 (−7.5, 16.8)	0.4 ± 0.3 (−0.3, 1.0)	0.3 ± 0.5 (−0.7, 1.3)
0.5	11.5 ± 8.5 (−5.1, 28.2)	0.9 ± 0.5 (−0.1, 1.8)	0.6 ± 0.5 (−0.5, 1.6)

Note.—Data are the mean bias ± standard deviations of the differences, with limits of agreement as 95% confidence intervals in parentheses.

of 0.864–0.917 ($P < .0001$). (Table 2). The differences showed a normal distribution and the paired t tests showed that the perfusion values for white matter and gray matter did not differ significantly between the reference and optimal settings ($P = .089–.923$, Table 2).

Discussion

Our current study showed that the total dose for the clinical CT perfusion protocol for patients with acute stroke can be reduced to 2.5 mSv with only minor effects on perfusion values. The maximum mean difference in perfusion values was less than 5% and no significant differences were found when the optimal dose was compared with the reference standard. This was a promising result, especially because no noise reduction techniques were applied. In addition to reduced exposure to harmful radiation for the patient, CT perfusion imaging performed at the radiation dose of CT angiography (and possibly lower) allows the possibility of simplifying the complete imaging workup of patients with acute stroke to only CT perfusion imaging with algorithmically derived CT and head CT angiographic results (6,7).

The maximum mean difference of 5% at 2.5 mSv is low in light of the reported reproducibility of CT perfusion imaging. Both the observer variability due to region-of-interest selection and the variability due to arterial-input-function and venous-output-function selection were reported to be higher in previous studies (16,17). On the basis of qualitative visual assessments of

Figure 3

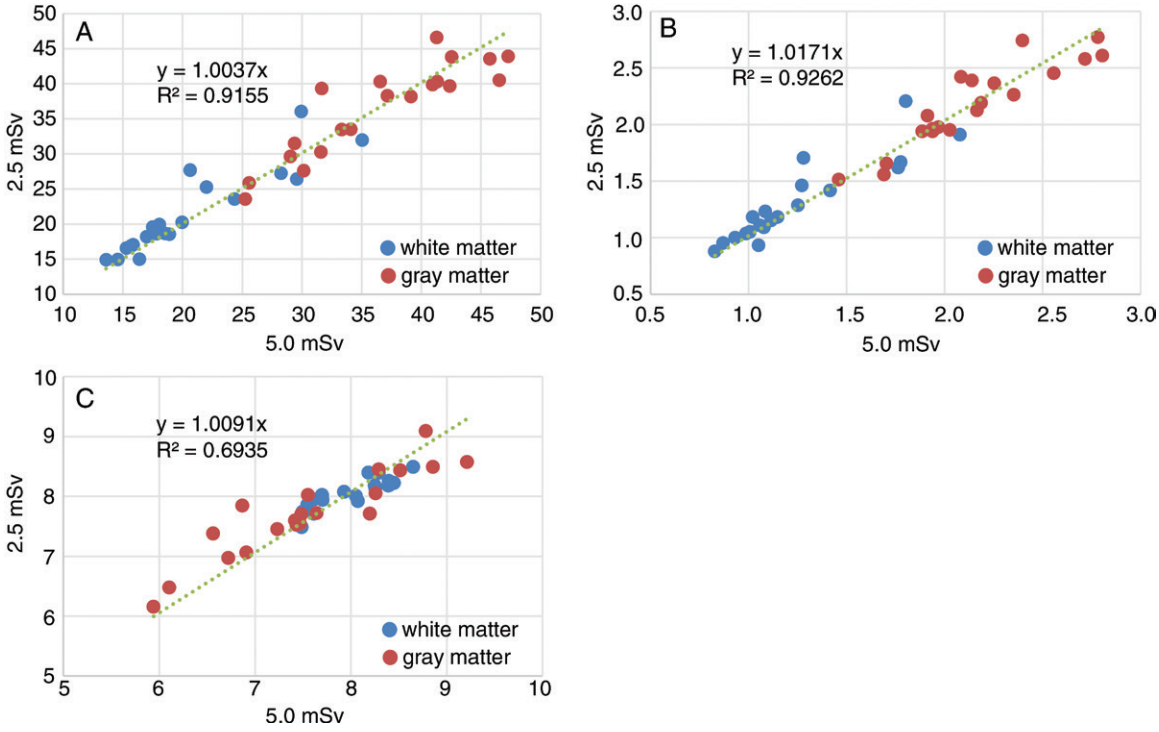

Figure 3: Scatterplots show patient perfusion values between reference standard (5.0 mSv) and optimal settings (2.5 mSv).

Table 2

Comparison of Perfusion Values at 5.0 mSv with those at 2.5 mSv

Brain Matter and Perfusion Value	Pearson Correlation		Shapiro-Wilk	Paired *t* Test
	r	*P* Value	*P* Value	*P* Value
White matter				
CBF	0.911	<.0001	.094	.118
CBV	0.906	<.0001	.025	.089
MTT	0.864	<.0001	.075	.371
Gray matter				
CBF	0.895	<.0001	.408	.923
CBV	0.917	<.0001	.094	.477
MTT	0.916	<.0001	.335	.118

Note.—All correlations were found to be significant, all differences followed a normal distribution, and no significant differences were found between the means (two-tailed tests, $P = .05$).

the CT perfusion maps, authors of two studies (18,19) reported that clinical decision making is unlikely to change if the overall variability stays within 10%.

Dose reduction to less than 2.5 mSv results in overestimation of patient perfusion values, particularly of CBF and CBV values. We hypothesize that increased noise levels lead to increased small-scale gradients on the intensity curves, which are erroneously interpreted as increased blood flow and volume during the deconvolution process inherent in the perfusion analysis. According to the central volume principle (20), MTT is less affected.

The fact that MTT values in our study were less affected than were CBF and CBV values when the dose was lowered is in concordance with the results of a study by Niesten et al (21) in which several types of reconstruction algorithms were compared when the total dose was decreased by one-half. Those authors found, however, that the CBV values of gray matter actually were underestimated by 18.6% in all patients, and the CBV values of white matter were overestimated by 1.5% with filtered back projection as the reconstruction algorithm, but they gave no explanation for this observation. Our optimal point of dose reduction was lower than the reduction of 33% (from 190 mAs to 125 mAs, no effective dose values were reported) suggested by Juluru et al (22). These authors found little effect of lower dose settings on perfusion values, although in their study, Juluru et al investigated five dose settings with simulated noise, whereas we used real measured noise.

To our knowledge, previously published work is limited primarily because of the difficulty of realistic simulation of patient data at different dose levels. In other studies, this was achieved by simply adding Gaussian noise (22), by reconstructing only a part of the total number of raw projections (21), or by using dual-source CT scanners and letting the two tubes operate at different milliampere and kilovolt settings simultaneously during acquisition (23). An alternative to our approach would be to use dedicated low-dose simulators (24,25). Our approach combined real patient tissue curves with multiple CT scans at a wide range of tube current settings to construct patient-specific digital phantoms. In van den Boom et al (14) these patient-specific phantoms were described and validated. Linear fits in the scatterplots of the perfusion values and corresponding digital phantoms yielded slope and R^2 values, respectively, of 1.03 and 0.96 for CBF, 1.06 and 0.97 for CBV, and 1.02 and 0.73 for MTT. Kudo et al (26) also used digital phantoms, but instead, they relied on simulated Gaussian noise and simulated general tissue curves. To our knowledge, our study is the first to quantitatively demonstrate the trends of perfusion values as a function of the total radiation dose of a clinical CT perfusion protocol.

Many factors have been identified that contribute to the variability of quantitative perfusion imaging (27,28); among them, scan parameters and software for doing the perfusion analysis. Kudo et al (29) showed significant differences among commercial software when identical source data were used. For this reason, we have used a freely available perfusion software package to ensure that the results of this study can be reproduced easily by other groups without the use of a vendor-specific workstation. In addition, other researchers can create digital phantoms such as those we used in this study by using instructions available at our digital phantom Web site (*http://digitalphantom.diagnijmegen.nl/*).

This study had some limitations. First, the sample size was relatively small, with tissue curves of only 20 patients included. However, the same trends were observed for all patients. Because the focus of the study was on radiation dose, for each patient and each percentage setting, 10 noise permutations of CT perfusion protocols were simulated, resulting in a total of 2000 four-dimensional simulations. Second, only perfusion values of regions of interest in normal-appearing white matter and basal ganglia were investigated. We kept all regions of interest in each patient constant during the experiments to avoid introducing another source of variation.

The next steps in this research are to simulate regions with infarcts at lower radiation doses, to assess diagnostic accuracy, and to apply optimized noise filters aimed at improved soft tissue contrast (30), angiographic imaging (31), or reconstruction algorithms (21,32,33).

In conclusion, CT perfusion imaging in patients with acute stroke is associated with high radiation dose, and the results of this study show the potential to lower the dose from 5.0 to 2.5 mSv for clinical CT perfusion protocols, with only minor quantitative effects on perfusion values.

Disclosures of Conflicts of Interest: R.M. Activities related to the present article: Grant (R0001366) from Toshiba Medical Systems, Japan. Activities not related to the present article: Grants/grants pending from the Dutch Technology Foundation (R0002376), Nuts-Ohra grant (R0001850). Other relationships: disclosed no relevant relationships. **M.T.H.O.** disclosed no relevant relationships. **B.v.G.** Activities related to the present article: Research grant from Toshiba. Activities not related to the present article: disclosed no relevant relationships. Other relationships: disclosed no relevant relationships. **M.P.** Activities related to the present article: Grant from Toshiba. Activities not related to the present article: payment for lectures from Bayer, Bracco, and Toshiba. Other relationships: disclosed no relevant relationships.

References

1. Jauch EC, Saver JL, Adams HP Jr, et al. Guidelines for the early management of patients with acute ischemic stroke: a guideline for healthcare professionals from the American Heart Association/American Stroke Association. Stroke 2013;44(3):870–947.
2. Vagal A, Meganathan K, Kleindorfer DO, Adeoye O, Hornung R, Khatri P. Increasing use of computed tomographic perfusion and computed tomographic angiograms in acute ischemic stroke from 2006 to 2010. Stroke 2014;45(4):1029–1034.
3. Mnyusiwalla A, Aviv RI, Symons SP. Radiation dose from multidetector row CT imaging for acute stroke. Neuroradiology 2009;51(10):635–640.
4. Diekmann S, Siebert E, Juran R, et al. Dose exposure of patients undergoing comprehensive stroke imaging by multidetector-row CT: comparison of 320-detector row and 64-detector row CT scanners. AJNR Am J Neuroradiol 2010;31(6):1003–1009.
5. Wintermark M, Lev MH. FDA investigates the safety of brain perfusion CT. AJNR Am J Neuroradiol 2010;31(1):2–3.
6. Smit EJ, Vonken EJ, van der Schaaf IC, et al. Timing-invariant reconstruction for deriving high-quality CT angiographic data from cerebral CT perfusion data. Radiology 2012;263(1):216–225.
7. Smit EJ, Vonken EJ, van Seeters T, et al. Timing-invariant imaging of collateral vessels in acute ischemic stroke. Stroke 2013;44(8):2194–2199.
8. Mettler FA Jr, Huda W, Yoshizumi TT, Mahesh M. Effective doses in radiology and diagnostic nuclear medicine: a catalog. Radiology 2008;248(1):254–263.
9. Klein S, Staring M, Murphy K, Viergever MA, Pluim JP. elastix: a toolbox for intensity-based medical image registration. IEEE Trans Med Imaging 2010;29(1):196–205.
10. Mendrik A, Vonken EJ, van Ginneken B, et al. Automatic segmentation of intracranial arteries and veins in four-dimensional cerebral CT perfusion scans. Med Phys 2010;37(6):2956–2966.
11. International Electrotechnical Commission. Particular requirements for the basic safety and essential performance of X-ray equipment for computed tomography. IEC 60601-2-44 ed3.0, 2014.
12. Saver JL. Time is brain—quantified. Stroke 2006;37(1):263–266.
13. Rohlfing T, Zahr NM, Sullivan EV, Pfefferbaum A. The SRI24 multichannel atlas of normal adult human brain structure. Hum Brain Mapp 2010;31(5):798–819.
14. van den Boom R, Manniesing R, Oei MT, et al. A 4D digital phantom for patient-specific simulation of brain CT perfusion protocols. Med Phys 2014;41(7):071907.

15. Wu O, Østergaard L, Weisskoff RM, Benner T, Rosen BR, Sorensen AG. Tracer arrival timing-insensitive technique for estimating flow in MR perfusion-weighted imaging using singular value decomposition with a block-circulant deconvolution matrix. Magn Reson Med 2003;50(1):164–174.

16. Waaijer A, van der Schaaf IC, Velthuis BK, et al. Reproducibility of quantitative CT brain perfusion measurements in patients with symptomatic unilateral carotid artery stenosis. AJNR Am J Neuroradiol 2007;28(5):927–932.

17. Soares BP, Dankbaar JW, Bredno J, et al. Automated versus manual post-processing of perfusion-CT data in patients with acute cerebral ischemia: influence on interobserver variability. Neuroradiology 2009;51(7):445–451.

18. Fiorella D, Heiserman J, Prenger E, Partovi S. Assessment of the reproducibility of postprocessing dynamic CT perfusion data. AJNR Am J Neuroradiol 2004;25(1):97–107.

19. Sanelli PC, Nicola G, Tsiouris AJ, et al. Reproducibility of postprocessing of quantitative CT perfusion maps. AJR Am J Roentgenol 2007;188(1):213–218.

20. Meier P, Zierler KL. On the theory of the indicator-dilution method for measurement of blood flow and volume. J Appl Physiol 1954;6(12):731–744.

21. Niesten JM, van der Schaaf IC, Riordan AJ, et al. Radiation dose reduction in cerebral CT perfusion imaging using iterative reconstruction. Eur Radiol 2014;24(2):484–493.

22. Juluru K, Shih JC, Raj A, et al. Effects of increased image noise on image quality and quantitative interpretation in brain CT perfusion. AJNR Am J Neuroradiol 2013;34(8):1506–1512.

23. Krissak R, Mistretta CA, Henzler T, et al. Noise reduction and image quality improvement of low dose and ultra low dose brain perfusion CT by HYPR-LR processing. PLoS ONE 2011;6(2):e17098.

24. Joemai RM, Geleijns J, Veldkamp WJ. Development and validation of a low dose simulator for computed tomography. Eur Radiol 2010;20(4):958–966.

25. Zabić S, Wang Q, Morton T, Brown KM. A low dose simulation tool for CT systems with energy integrating detectors. Med Phys 2013;40(3):031102.

26. Kudo K, Christensen S, Sasaki M, et al. Accuracy and reliability assessment of CT and MR perfusion analysis software using a digital phantom. Radiology 2013;267(1):201–211.

27. Goyal M, Menon BK, Derdeyn CP. Perfusion imaging in acute ischemic stroke: let us improve the science before changing clinical practice. Radiology 2013;266(1):16–21.

28. Lev MH. Perfusion imaging of acute stroke: its role in current and future clinical practice. Radiology 2013;266(1):22–27.

29. Kudo K, Sasaki M, Yamada K, et al. Differences in CT perfusion maps generated by different commercial software: quantitative analysis by using identical source data of acute stroke patients. Radiology 2010;254(1):200–209.

30. Mendrik AM, Vonken EJ, van Ginneken B, et al. TIPS bilateral noise reduction in 4D CT perfusion scans produces high-quality cerebral blood flow maps. Phys Med Biol 2011;56(13):3857–3872.

31. Manniesing R, Viergever MA, Niessen WJ. Vessel enhancing diffusion: a scale space representation of vessel structures. Med Image Anal 2006;10(6):815–825.

32. Lin CJ, Wu TH, Lin CH, et al. Can iterative reconstruction improve imaging quality for lower radiation CT perfusion? Initial experience. AJNR Am J Neuroradiol 2013;34(8):1516–1521.

33. Komlosi P, Zhang Y, Leiva-Salinas C, et al. Adaptive statistical iterative reconstruction reduces patient radiation dose in neuroradiology CT studies. Neuroradiology 2014;56(3):187–193.